Special Collection

Toward Continuous-Flow Hyperpolarisation of Metabolites via Heterogenous Catalysis, Side-Arm-Hydrogenation, and Membrane Dissolution of Parahydrogen

William G. Hale,[a] Tommy Y. Zhao,[a] Diana Choi,[a] Maria-Jose Ferrer,[a] Bochuan Song,[b] Hanqin Zhao,[b] Helena E Hagelin-Weaver,[b] and Clifford R. Bowers*[a, c]

Side-arm hydrogenation (SAH) by homogeneous catalysis has extended the reach of the parahydrogen enhanced NMR technique to key metabolites such as pyruvate. However, homogeneous hydrogenation requires rapid separation of the dissolved catalyst and purification of the hyperpolarised species with a purity sufficient for safe in-vivo use. An alternate approach is to employ heterogeneous hydrogenation in a continuous-flow reactor, where separation from the solid catalysts is straightforward. Using a TiO_2-nanorod supported Rh catalyst, we demonstrate continuous-flow parahydrogen enhanced NMR by heterogeneous hydrogenation of a model SAH precursor, propargyl acetate, at a flow rate of 1.5 mL/min. Parahydrogen gas was introduced into the flowing solution phase using a novel tube-in-tube membrane dissolution device. Without much optimization, proton NMR signal enhancements of up to 297 (relative to the thermal equilibrium signals) at 9.4 Tesla were shown to be feasible on allyl-acetate at a continuous total yield of 33%. The results are compared to those obtained with the standard batch-mode technique of parahydrogen bubbling through a suspension of the same catalyst.

Nuclear magnetic resonance (NMR) spectroscopy is a non-invasive and non-destructive analytical technique that has found applications in many fields of science, but it suffers from inherently low sensitivity. Fortunately, the sensitivity problem can be addressed by hyperpolarisation methods. Among them, parahydrogen enhanced polarisation[1,2] offers comparatively lower cost, greater reliability and simplicity, and higher throughput. Para-enriched H_2 (pH_2) can be stored for many weeks and still produce hyperpolarised molecules and can be used in gas phase as well as liquid phase reactions. Side-arm hydrogenation (SAH) is a promising recent advancement that extends the reach of the parahydrogen-based methodology. To provide a means of incorporating parahydrogen into a carboxylic acid metabolite of interest, an unsaturated side-arm (e.g propargyl) is attached to it via an ester linkage. After hydrogenating the side-arm with pH_2, the proton hyperpolarisation can be transferred across the ester linkage to the carbonyl ^{13}C.[3–6] The side-arm is subsequently cleaved by hydrolysis, releasing the hyperpolarised metabolite.[5,7,8] SAH by homogeneous hydrogenation catalysis has been used to produce acetate and pyruvate, the latter being a key marker in the Warburg effect.[4,9]

In liquid phase batch mode experiments, pH_2 is typically introduced by bubbling through a solution containing the substrate and a dissolved or suspended catalyst. Continuous flow (CF) SABRE and PASADENA have been demonstrated using gas bubbling[10] as a means of dissolution. However, the rapid separation of the hyperpolarised metabolite produced by homogeneous catalysis with purity sufficient for in-vivo use is a significant challenge.[11] CF hyperpolarisation from pH_2 and heterogeneous catalysis, whereby hyperpolarised product molecules are produced in a stream, would offer several key advantages over batch mode processes: uninterrupted production with consistent yield and polarisation, ease of catalyst regeneration, and spontaneous separation of the hyperpolarised products from the solid catalyst material. While CF heterogeneous hydrogenation is intrinsically compatible with the production of hyperpolarised gases, some modifications are necessary when operating with liquids. Firstly, a method for dissolution of pH_2 that does not generate gas bubbles is needed. In batch mode experiments in liquids, the pH_2 bubbling must be interrupted prior to data acquisition because bubbles cause magnetic susceptibility mismatches within the sample that spoil field homogeneity and spectral quality, making structure elucidation and quantification of products impossible. Continuous flow dissolution of gases for a reaction can be achieved using a membrane that is permeable to the gas but not the liquid, and parahydrogen enhanced NMR by homogeneous catalysis has been successfully demonstrated using this approach.[12–14]

The *tube-in-tube* membrane design developed by O'Brien and co-workers was demonstrated as a safe and bubble-free way to dissolve hydrogen at elevated pressures (~25 bar). They used an outer tube made of PTFE that is filled with hydrogen

[a] Dr. W. G. Hale, T. Y. Zhao, D. Choi, M.-J. Ferrer, Prof. C. R. Bowers
Department of Chemistry
University of Florida
Gainesville, Florida, 32611
E-mail: russ@ufl.edu
[b] B. Song, H. Zhao, Prof. H. E Hagelin-Weaver
Department of Chemical Engineering
University of Florida
Gainesville, Florida, 32611
[c] Prof. C. R. Bowers
National High Magnetic Field Laboratory
Gainesville, Florida, 32611

Supporting information for this article is available on the WWW under https://doi.org/10.1002/cphc.202100119

Special Collection An invited contribution to a Special Collection on Parahydrogen Enhanced Resonance

and an inner tube of Teflon AF2400 containing the flowing liquid. The high permeability of H_2 in AF2400 means that it quickly diffuses through and dissolves into the liquid. Similar designs have since been used in organic synthesis for both heterogeneous and homogeneous catalysis.[15–18] Recently, Tijssen *et al.* adapted the tube-in-tube set-up for use with a microfluidic NMR probe.[19] Using the membrane dissolution device, they monitored the hydrogenation of various compounds using palladium microencapsulated in polyurea as a heterogeneous catalyst in continuous flow. However, no para-hydrogen enhanced signals were observed, probably due to the catalyst being unsuitable.[19]

Heterogeneously catalysed PASADENA, ALTADENA, and SWAMP have been reported using liquid substrates[20–25] with several types of catalysts. Glöggler and co-workers have used ligand stabilised nanoparticles[7,24,26] to hyperpolarise amino acids and other biologically relevant molecules. While outstanding polarisation levels were achieved, the problem of removing the nanoparticles from the reaction mixture is similar to that of homogeneous catalysis. Kovtunov *et al.* have described titania supported metal catalysts capable of producing hyperpolarised metabolites,[22,23] and Zhao *et al.* reported hyperpolarisation of 2-hydroxyethyl propionate in water using $Pt_3Sn@mSiO_2$ intermetallic nanoparticles stabilised inside mesoporous silica.[21] In batch mode experiments, the heavy catalyst particles showed spontaneous rapid settling of the catalyst after cessation of bubbling, affording background levels of Pt and Sn of only 15 and 70 ppb, respectively. However, to our knowledge, CF hyperpolarisation of a liquid by heterogeneous catalysis with pH_2 has not been reported previously.

Here we demonstrate CF ALTADENA (Adiabatic Longitudinal Transport After Dissociation Engenders Net Alignment) by heterogeneous hydrogenation of propargyl acetate (i.e. a side-arm modification of acetate) in methanol-d_4 utilising a tube-in-tube reactor system consisting of a hydrogen permeable membrane tubing; a temperature controlled flow-through packed bed catalytic reactor; and a Varian micro-flow NMR probe. The reactor was packed with 25 mg of Rh nanoparticles supported on rod-shaped TiO_2 nanocrystals (0.5 wt%). The Rh loading is ~40 times lower than the loading on the Rh/TiO_2 catalysts used in previous liquid phase SAH experiments.[23] Consistent with the light-off curve for hydrogenation of ethylene (Figure S2 in the SI), this Rh catalyst exhibited efficient hydrogenation even at room temperature. The pH_2 adducts

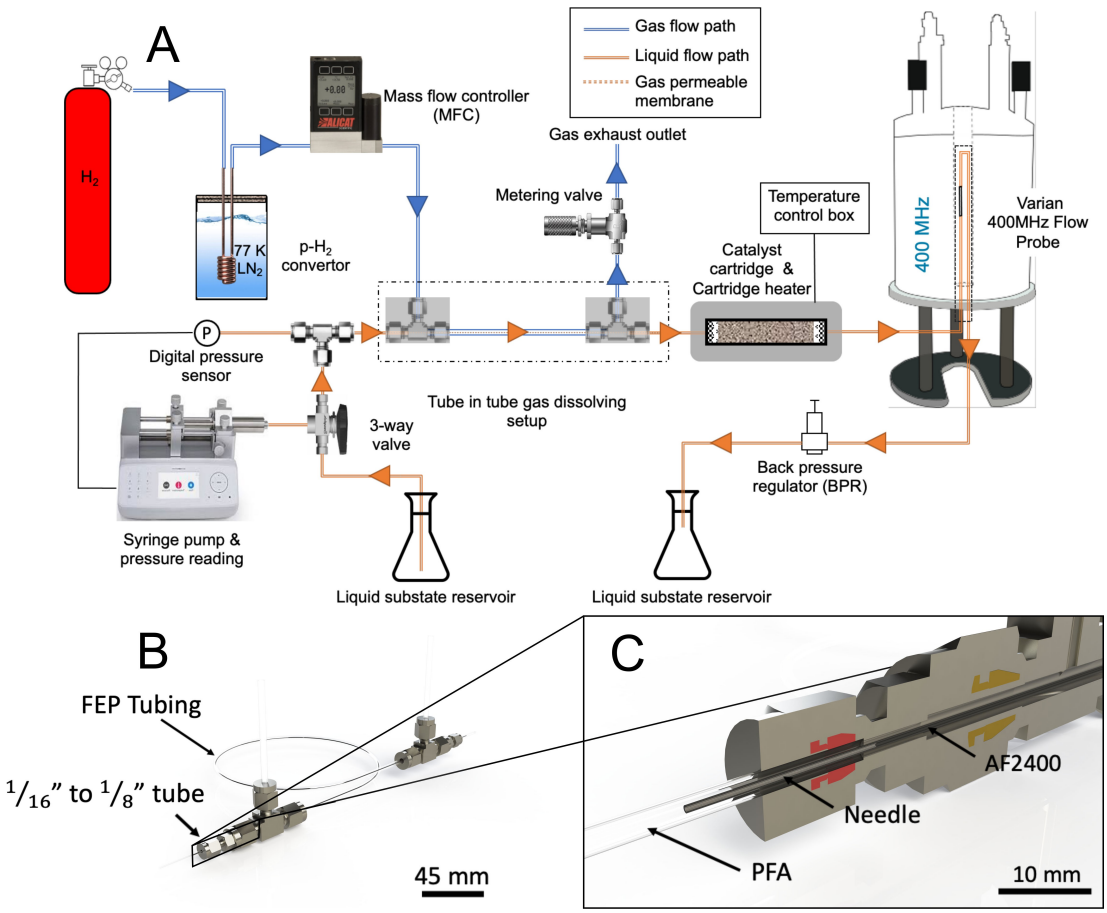

Figure 1. (A) Experimental set-up. The liquid is drawn into the syringe from the left liquid reservoir and the 3-way valve is then changed to allow the liquid to flow through the tube-in-tube and then into the heated catalyst cartridge. The liquid flows into the magnet for detection and is collected into a separate reservoir. (B) Rendering of the tube-in-tube device. (C) Close up of the liquid inlet port showing the PFA (clear) tubing, 316 stainless steel needle (grey), and AF2400 membrane 'inner tube' (black).

were formed in the ~5 Gauss fringe field of the NMR magnet. The hyperpolarised allyl acetate (AA) and propyl acetate (PPA) then flowed into the NMR probe for detection at 9.4 T, corresponding to the ALTADENA conditions, yielding in-phase multiplets in pure absorption or emission phase (in the weak coupling regime).[27]

Our CF heterogeneous hydrogenation setup is illustrated in Figure 1. A Chemyx 6000 syringe pump was used to generate liquid flow at a constant flow rate. A digital pressure sensor is connected to the pump outlet to monitor the liquid pressure. Hydrogen gas is introduced into the tube-in-tube gas dissolution device through a Swagelok Tee. The tube-in-tube device is based on previous designs[15,19] with renderings shown in Figure 1. Details of its construction are provided in the SI.

After dissolution of pH_2 in the tube-in-tube device, the reaction mixture flows into the catalytic reactor cartridge enclosed in a temperature-controlled brass block, as illustrated in Figure 2. The granular catalyst material is confined between two IDEX™ disk filters with 10-micron pore size. The filters were backed with glass wool to prevent clogging. The reactor effluent flows through approximately 15 cm of PEEK tubing (OD = 1.59 mm, ID = 0.76 mm) into the inlet port of the 400 MHz flow probe (Varian SN172, 400 MHz, 60 μL detection volume) for NMR detection. A 2.75 bar back-pressure regulator at the outlet of the flow probe prevents degassing and bubble formation inside the probe.

Propargyl acetate (PPGA) was chosen as the substrate for our initial demonstration as it has already been successfully demonstrated as a SAH precursor.[3] The reaction scheme is included at the top of Figure 3. An arrayed experiment was performed with collection of a spectrum using a $\pi/2$ pulse every 10 seconds for 300 s. The syringe was stopped after collection of the 24th spectrum and the data acquisition continued for another 60 s. A stacked plot of the resulting spectra is presented in Figure 3. Upon activating the syringe pump, the CF-ALTADENA peaks of both AA and PPA are seen to grow in after about 100 s as these hyperpolarised products reach the NMR detection coil. Over the same period, the unreacted propargyl acetate peaks are seen to decrease due to incomplete thermal equilibration at high field. This is because the transport time to high field is somewhat shorter than the T_1 relaxation time under flowing conditions. When the syringe was stopped, the ALTADENA peaks are seen to gradually disappear, while the peaks arising from high-field thermal polarisation are seen to grow. During the steady-state condition (scans 12–24), the CF-ALTADENA signals of both AA and PPA are remarkably stable and reproducible over a period of several minutes. When the syringe pump stops, the rate of fluid flow through the NMR coil does not stop instantaneously due to equilibration of the pressure. The gradual decay of the ALTADENA signals corresponds to the gradual reduction in the actual flow.

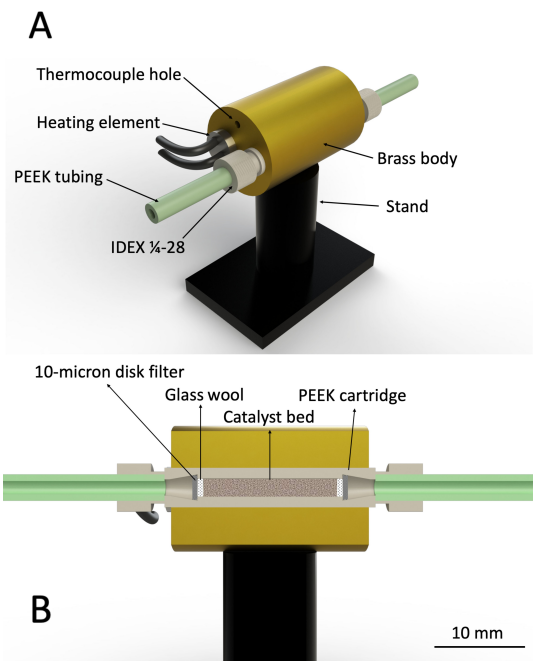

Figure 2. (A) Rendering of the catalyst cartridge, heating element, and heating block. (B) A cut-through rendering showing the make-up of the catalyst cartridge.

Figure 4 shows the signal-averaged thermally polarised spectrum (in grey) acquired 1 minute after the end of the arrayed experiment overlayed with a representative CF-ALTADENA spectrum (in blue) from the steady-state regime. A quantitative analysis of the signal enhancement factor was performed by comparing the ALTADENA spectrum to the thermally polarised spectrum. Details of the calculations of the enhancement factor and conversion are provided in the SI. Using 50% pH_2, a 50.1-fold enhancement was achieved at the H_f proton of AA and a 47.2-fold enhancement was achieved at the H_i proton in PPA. Note that had the experiments been performed using 100% para-enrichment, all of the signal enhancements would have been approximately three times greater.[28]

A limited optimisation of the CF ALTADENA experimental conditions was performed by conducting the hydrogenation at several different flow rates and temperatures. The effect of temperature was studied at two different temperatures, 50 °C and 80 °C, while keeping the liquid flow rate constant at 1.5 mL/min, and the results are shown in Figure 4. The observed enhancements measured for the H_f proton at 50 °C and 80 °C were 50.1 and 63.5 respectively with conversions of 15.3% and 19.1%. These enhancements are believed to be significantly reduced by the spin-lattice relaxation of the hyperpolarised product molecules during the 4.9 s transportation of the liquid from the catalyst cartridge to the sensitive volume inside the NMR probe. Intrinsic enhancement factors, obtained by applying a correction factor to account for spin relaxation, are reported in the SI. To directly compare the amount of hyperpolarised signal generated in the experiments, an *enhancement yield* was obtained by taking the product of the observed enhancement factor and the conversion. This demonstrates that the experiment at 80 °C generates 58% more hyperpolarised signal than at 50 °C, although there is only 27% difference in terms of enhancement factor.

As 80 °C gave the higher enhancement, the flow rate dependence of the reaction was studied at this temperature.

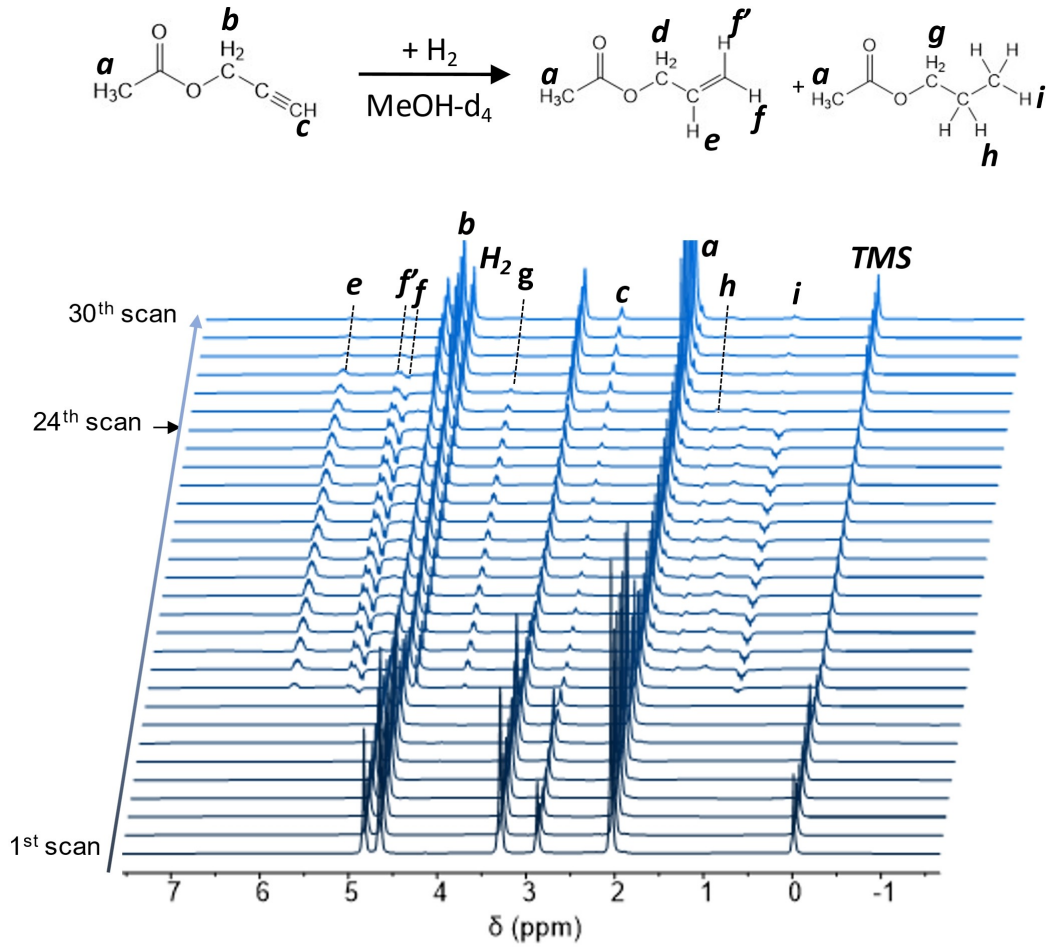

Figure 3. Stacked 400 MHz ^{1}H ALTADENA spectra acquired over the course of a continuous flow experiment using a reactor temperature of 50 °C and a flow rate of 1.5 mL/min. The syringe pump is started at the first scan and stopped at the 24th scan. Spectra were acquired in 10 second increments.

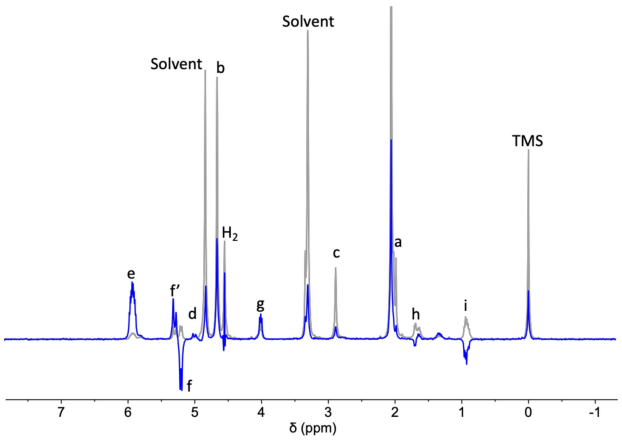

Figure 4. ^{1}H ALTADENA spectrum (Blue, 1 scan) and thermally polarised spectrum (Grey, 16 scans, d1 = 30 s) acquired for the liquid phase continuous flow propargyl acetate hydrogenation catalysed by Rh/TiO_2 at 80 °C and 1.5 mL/min.

Shown in Figure S7(B) and S7(C) in the SI are the ALTADENA and thermal equilibrium spectra obtained using flow rates of 1.5 mL/min and 2.0 mL/min respectively. The enhancements measured for the H_f proton were 63.5 at 1.5 mL/min and 63.6 for 2.0 mL/min. The results are summarized in Table 1. As one increases the flow rate, the transfer time decreases, meaning less time for the hyperpolarised species to relax before it reaches the detection coil of the probe. However, as the flow rate increases, the catalyst contact time (i.e., the length of time the solution resides in the catalyst cartridge) decreases, resulting in decreased formation of hyperpolarised product. These experimental parameters do not appear to have an equal effect. As the conversion increases from 9.15% to 19.1% when decreasing flow rate and the transport time goes from 3.66 s to 4.88 s, this ~50% difference in product formed is compensated by only a 33% difference in the transfer time. This indicates that the relaxation of the hyperpolarised product is the dominant effect in these experiments.

For comparison, batch mode ALTADENA experiments were performed using the same temperature, substrate concentration, catalyst, and catalyst mass (details in SI) as in the CF experiments. Unlike the CF ALTADENA experiments, the hydrogenation reaction continues even after the bubbling has been

Table 1. A summary of the best results obtained from a continuous flow experiment. Results for all reaction conditions are included in the SI.

Conditions	Conversion PPGA→AA	Conversion PPGA→PPA	Enhancement AA, H_f	Enhancement PPA, H_i	Enhancement yield* AA, H_f	Enhancement yield* PPA, H_i
80 °C 1.5 mL/ min	19.1 % ± 0.3 %	13.6 % ± 0.2 %	63.5 ± 1.8	44.2 ± 0.9	12.1 ± 0.5	6.0 ± 0.3

stopped. In the batch mode experiments, spectra were collected with a $\pi/2$ pulse every 3 s after inserting the NMR tube into the probe until no ALTADENA signals could be observed. These spectra were then summed to give the total ALTADENA signal. The measured enhancement factors for the three trials varied considerably, with a maximum of 30.5 and an average of 19.2. The average conversions from PPGA to AA and PPGA to PPA were 37.5 % and 24.7 % respectively, whilst the enhancement on H_f and H_i from AA was 19.2, and 8.6, respectively. The transport time in these manual transfer ALTADENA "bubble-and-drop" experiments was about 7 s. Hence, the enhancements were subject to roughly 20 % greater spin-lattice relaxation losses than the CF experiments where the transport time was 4.9 s. On the other hand, the batch mode spectra were collected at 300 MHz, and so these signal enhancements should be multiplied by a factor of 3/4 before comparison to those obtained in the CF experiments at 400 MHz. After taking into account both factors, we find that the CF experiment using tube-in-tube dissolution of pH_2 yielded significantly higher signal enhancements than the batch mode ALTADENA process.

Future work will entail further optimization of the signal enhancement, conversion, and yield through a more comprehensive exploration of the parameter space. At present, the experiments are restricted by the pressures generated within the catalyst cartridge and the volume between catalyst cartridge and the sensitive volume in the NMR detection coil which limits the flow rates and transport times that can be realized. As this volume is dominated by the internal volume of the probe, the transfer time dominates the polarisation losses. A pulsed transfer, where reactants emerging from the catalytic reactor are rapidly shuttled to the detection field, could mitigate these relaxation losses. Higher enhancement factors might also be achieved by improved catalyst cartridge design to facilitate lower pressures at higher flow rates and simultaneously increased catalyst contact time.

To summarize, we have demonstrated the feasibility of CF hyperpolarisation by heterogeneous hydrogenation of a solution-state SAH precursor, propargyl acetate. A key advantage of continuous-flow heterogeneous catalysis is its inherent compatibility with flow-chemistry. NMR signal enhancement factors of up to 64 were observed using 50 % para enriched H_2 at 400 MHz. Had 100 % pH_2 been used, an enhancement of 192 would have been observed, and the intrinsic enhancement factor, after correction for spin relaxation losses, would have been approximately 300. Furthermore, a substantial total conversion of 33 % was obtained in the continuous-flow hydrogenation using only 25 mg of the 0.5 wt % TiO_2-nanorod supported Rh catalyst with membrane dissolution of pH_2. While methanol-d_4 was chosen as the solvent for this initial demonstration, the crucial next step will be to perform the hydrogenation in a biocompatible solvent (i.e. D_2O), which could prove to be a transformative development for in-vivo spectroscopy and imaging applications.

Acknowledgements

Financial support was received from NSF grants CHE-1808239, CBET-1933723, and the National High Magnetic Field Laboratory's User Collaborative Grant Program, which is supported by the National Science Foundation Cooperative Agreement No. DMR-1644779 and the State of Florida.*

Conflict of Interest

The authors declare no conflict of interest.

Keywords: Hyperpolarisation · parahydrogen · heterogeneous catalysis · hydrogenation · membrane reactor

[1] C. R. Bowers, D. P. Weitekamp, *J. Am. Chem. Soc.* **1987**, *109*, 5541–5542.
[2] C. R. Bowers, D. P. Weitekamp, *Phys. Rev. Lett.* **1986**, *57*, 2645–2648.
[3] F. Reineri, T. Boi, S. Aime, *Nat. Commun.* **2015**, *6*, 1–6.
[4] E. Cavallari, C. Carrera, S. Aime, F. Reineri, *ChemPhysChem* **2019**, *20*, 318–325.
[5] L. Dagys, A. P. Jagtap, S. Korchak, S. Mamone, P. Saul, M. H. Levitt, S. Glöggler, *Analyst* **2021**, DOI 10.1039/D0AN02389B.
[6] S. Korchak, S. Mamone, S. Glöggler, *ChemistryOpen* **2018**, *7*, 672–676.
[7] L. Kaltschnee, A. P. Jagtap, J. McCormick, S. Wagner, L. Bouchard, M. Utz, C. Griesinger, S. Glöggler, *Chem. Eur. J.* **2019**, *25*, 11031–11035.
[8] S. Korchak, S. Mamone, S. Glöggler, *ChemistryOpen* **2018**, *7*, 672–676.
[9] M. V. Liberti, J. W. Locasale, *Trends Biochem. Sci.* **2016**, *41*, 211–218.
[10] P. Štěpánek, C. Sanchez-Perez, V. V. Telkki, V. V. Zhivonitko, A. M. Kantola, *J. Magn. Reson.* **2019**, *300*, 8–17.
[11] J. Eills, E. Cavallari, C. Carrera, D. Budker, S. Aime, F. Reineri, *J. Am. Chem. Soc.* **2019**, *141*, 20209–20214.
[12] S. Lehmkuhl, M. Wiese, L. Schubert, M. Held, M. Küppers, M. Wessling, B. Blümich, *J. Magn. Reson.* **2018**, *291*, 8–13.
[13] L. Bordonali, N. Nordin, E. Fuhrer, N. MacKinnon, J. G. Korvink, *Lab Chip* **2019**, *19*, 503–512.
[14] J. Eills, W. Hale, M. Sharma, M. Rossetto, M. H. Levitt, M. Utz, *J. Am. Chem. Soc.* **2019**, *141*, 9955–9963.
[15] M. O'Brien, N. Taylor, A. Polyzos, I. R. Baxendale, S. V. Ley, *Chem. Sci.* **2011**, *2*, 1250–1257.
[16] M. Brzozowski, M. O'brien, S. V Ley, A. Polyzos, *Acc. Chem. Res.* 2015, DOI 10.1021/ar500359m.
[17] E. Dimitriou, R. H. Jones, R. G. Pritchard, G. J. Miller, M. O'Brien, *Tetrahedron* **2018**, *74*, 6795–6803.
[18] B. Venezia, L. Panariello, D. Biri, J. Shin, S. Damilos, A. N. P. Radhakrishnan, C. Blackman, A. Gavriilidis, *Catal. Today* **2020**, *362*, 104–112.

[19] K. C. H. Tijssen, B. J. A. Van Weerdenburg, H. Zhang, J. W. G. Janssen, M. C. Feiters, P. J. M. Van Bentum, A. P. M. Kentgens, *Anal. Chem.* **2019**, *91*, 12636–12643.
[20] L. B. Bales, K. V. Kovtunov, D. A. Barskiy, R. V. Shchepin, A. M. Coffey, L. M. Kovtunova, A. V. Bukhtiyarov, M. A. Feldman, V. I. Bukhtiyarov, E. Y. Chekmenev, I. V. Koptyug, B. M. Goodson, *J. Phys. Chem. C* **2017**, *121*, 15304–15309.
[21] E. W. Zhao, R. Maligal-Ganesh, C. Xiao, T.-W. Goh, Z. Qi, Y. Pei, H. E. Hagelin-Weaver, W. Huang, C. R. Bowers, *Angew. Chem.* **2017**, *129*, 3983–3987; *Angew. Chem. Int. Ed.* **2017**, *56*, 3925–3929.
[22] K. V Kovtunov, V. V Zhivonitko, I. V Skovpin, D. A. Barskiy, O. G. Salnikov, I. V. Koptyug, *J. Phys. Chem. C* **2013**, *117*, 22887–22893.
[23] K. V. Kovtunov, D. A. Barskiy, R. V. Shchepin, O. G. Salnikov, I. P. Prosvirin, A. V. Bukhtiyarov, L. M. Kovtunova, V. I. Bukhtiyarov, I. V. Koptyug, E. Y. Chekmenev, *Chem. Eur. J.* **2016**, *22*, 16446–16449.
[24] J. McCormick, S. Korchak, S. Mamone, Y. N. Ertas, Z. Liu, L. Verlinsky, S. Wagner, S. Glöggler, L. Bouchard, *Angew. Chem.* **2018**, *130*, 10852–10856; *Angew. Chem. Int. Ed.* **2018**, *57*, 10692–10696.
[25] E. W. Zhao, R. Maligal-Ganesh, Y. Du, T. Y. Zhao, J. Collins, T. Ma, L. Zhou, T. W. Goh, W. Huang, C. R. Bowers, *Chem* **2018**, *4*, 1387–1403.
[26] S. Glöggler, A. M. Grunfeld, Y. N. Ertas, J. McCormick, S. Wagner, P. P. M. Schleker, L.-S. Bouchard, *Angew. Chem. Int. Ed.* **2015**, *54*, 2452–2456; *Angew. Chem.* **2015**, *127*, 2482–2486.
[27] M. G. Pravica, D. P. Weitekamp, *Chem. Phys. Lett.* **1988**, *145*, 255–258.
[28] Y. Du, R. Zhou, M. J. Ferrer, M. Chen, J. Graham, B. Malphurs, G. Labbe, W. Huang, C. R. Bowers, *J. Magn. Reson.* **2020**, *321*, 106869.

Manuscript received: February 13, 2021
Revised manuscript received: March 9, 2021
Accepted manuscript online: March 10, 2021